On the synthesis and structure of LaCaGaO$_4$

Zhaofei Li, Guobao Li,* Fuhui Liao, and Jianhua Lin*

State Key Laboratory of Rare Earth Materials Chemistry and Applications, College of Chemistry and Molecular Engineering, Peking University, Beijing 100871, People's Republic of China

Abstract

The phase relationship of the La$_2$O$_3$–CaO–Ga$_2$O$_3$ system at 1150°C has been studied and is expressed in a phase-diagram, in which the presence of two ternary compounds were confirmed. The ternary compound LaCaGaO$_4$ has two forms, i.e., the orthorhombic (o-) phase and the tetragonal (t-) phase. Both phases are isolators exhibiting ferroelectric behavior, so the structures were reformulated in the polar space groups.
© 2002 Elsevier Science (USA). All rights reserved.

1. Introduction

Gallium perovskite LaGaO$_3$-based materials have attracted much attention in recent years [1–11] because of their extraordinary oxygen-ion conductivity. It was suggested that LaGaO$_3$ has optimized structure parameters in the perovskite family to obtain large ionic conductivity [11]; this was indeed realized experimentally in many LaGaO$_3$ systems [12]. Accordingly, a number of related systems, such as La$_2$O$_3$–SrO–Ga$_2$O$_3$ [13], La$_2$O$_3$–MgO–Ga$_2$O$_3$ [13], La$_2$O$_3$–NiO–Ga$_2$O$_3$ [14], La$_2$O$_3$–CeO$_2$–Ga$_2$O$_3$ [15], have been studied. Most of these studies focussed on improving the performance of the LaGaO$_3$-based materials. On the other hand, the structural chemistry of gallium (III) is resemblance to aluminum analogues that exhibit both octahedral and tetrahedral coordination by oxygen atoms. For example, many compounds with general formula $LnMA$O$_4$ (Ln = rare earth, M = Ba, Sr, Ca, A = Ga, Al) [16–31] were reported as the potential substrates for thin-film high-T_c superconductors [32–34]. A majority of them crystallize in the K$_2$NiF$_4$-type structure in the tetragonal space group $I4/mmm$ [32]. In these compounds, the gallium atoms are octahedrally coordinated and the rare earth and alkaline earth atoms randomly occupy the other cation sites. $LnMA$O$_4$ can also crystallize in olivine-type structure, in which the gallium or aluminum

is tetrahedrally coordinated and, the rare earth and alkaline earth cations are ordered in different crystallographic sites [27,28,32,35]. In this paper, we examine the phase relationship of the La$_2$O$_3$–CaO–Ga$_2$O$_3$ system. Because both t-LaCaGaO$_4$ and o-LaCaGaO$_4$ exhibit ferroelectric property, their structures were reformulated in the polar space groups.

2. Experimental

All of the samples in the La$_2$O$_3$–CaO–Ga$_2$O$_3$ system were prepared by using conventional high-temperature reaction. The starting materials were dried before use. La$_2$O$_3$ (99.99%) and Ga$_2$O$_3$ (A.R.) were heated at 1150°C for 12 h, and CaCO$_3$ (A.R.) was dried at 200°C. The stoichiometric starting materials were mixed and preheated at 900°C and then at 1000°C for 2 h. The samples were then sintered at 1150°C in air for a week with repeated intermediate grinding and pressing. The products are all colorless polycrystalline powders. The tetragonal and orthorhombic LaCaGaO$_4$ samples were synthesized by similar procedure but with different annealing processes. The o-LaCaGaO$_4$ was obtained by cooling the sample slowly along with the furnace. The t-LaCaGaO$_4$ was obtained by further heating the phase-pure o-LaCaGaO$_4$ sample at 1350°C in air for about 1 min and then air-quenching to room temperature.

The chemical analyses were carried out with inductively coupled plasma atomic emission spectroscopy on a Leeman Labs Profile Spec ICP-AES. Powder X-ray

*Corresponding authors. Fax: +8610-62751708.

E-mail addresses: gbli@chem.pku.edu.cn (G. Li), jhlin@chem.pku.edu.cn (J. Lin).

diffraction were recorded using a Rigaku D/Max-2000 diffractometer with graphite monochromatized $CuK\alpha$ radiation at 50 kV, 200 mA. Powder-diffraction data used for structure refinement were collected in the range of 10–120° with step scanning mode. Rietveld refinement, using GSAS program [36], has been performed to analyze the crystal structure. In situ X-ray diffraction patterns at temperatures between 27°C and 1255°C were measured using a Brucker D8 Advance diffractometer with $CuK\alpha_1$ radiation at 40 kV and 40 mA. AC impedance of the samples pasted with Pt was measured with a HP4192A impedance analyzer in the frequency range from 1 kHz to 12 MHz between 400°C and 800°C. The electric hysteresis loops were measured on a ferroelectric tester (RT6000HVS by Radiant Technology Inc., USA) at room temperature.

3. Results and discussion

Fig. 1 shows the phase diagram at 1150°C and distribution of the tested compositions in the La_2O_3–CaO–Ga_2O_3 system. The corresponding details are listed in Table 1.

The stable phases at the apices of the ternary phase diagram are CaO, La_2O_3 and Ga_2O_3. No intermediate phase is present in the binary La_2O_3–CaO. Two binary compounds, $LaGaO_3$ [10] and $La_4Ga_2O_9$ [37], were confirmed in the binary La_2O_3–Ga_2O_3 [13–15]. The reported $LaGa_3O_6$ [38] was not confirmed in the phase diagram at 1150°C. Four compounds, $Ca_5Ga_6O_{14}$ [39,40], $Ca_3Ga_4O_9$ [41], $CaGa_2O_4$ [42], and $CaGa_4O_7$ [42], were confirmed to be stable at 1150°C in the binary CaO–Ga_2O_3. The existence of $Ca_3Ga_2O_6$ [42] at 1150°C has not been confirmed.
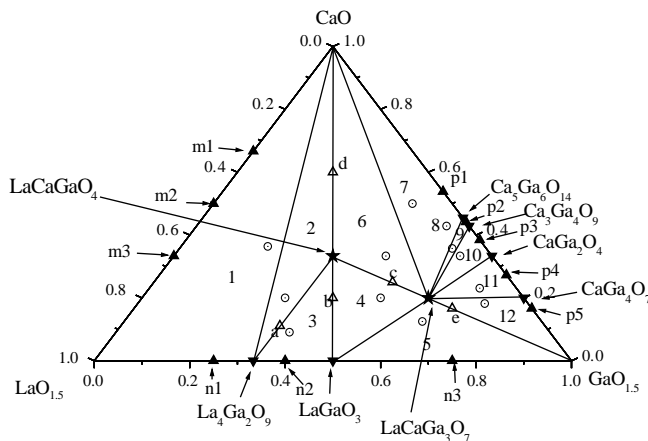

Fig. 1. Phase diagram of La_2O_3–CaO–Ga_2O_3 at 1150°C. (★) the ternary compound; (▼) the binary compounds; (▲, △), the two phases mixture; (⊙) the three phases mixture.

Table 1
Results of X-ray powder diffraction analyses of some compositions in the La_2O_3–CaO–Ga_2O_3 system at 1150°C in air

| No	Symbol	Compositions	Phase identified
1	⊙	$5.0LaO_{1.5} + 4.0CaCO_3 + 2.0GaO_{1.5}$	$La_2O_3 + CaO + La_4Ga_2O_9$
2	⊙	$5.0LaO_{1.5} + 2.0CaCO_3 + 3.0GaO_{1.5}$	$CaO + La_4Ga_2O_9 + LaCaGaO_4$
3	⊙	$3.0LaO_{1.5} + 0.5CaCO_3 + 2.0GaO_{1.5}$	$La_4Ga_2O_9 + LaGaO_3 + LaCaGaO_4$
4	⊙	$3.0LaO_{1.5} + 2.0CaCO_3 + 5.0GaO_{1.5}$	$LaCaGaO_4 + LaCaGa_3O_7 + LaGaO_3$
5	⊙	$2.0LaO_{1.5} + 1.0CaCO_3 + 5.0GaO_{1.5}$	$LaGaO_{3+} Ga_2O_3 + LaCaGa_3O_7$
6	⊙	$2.0LaO_{1.5} + 3.0CaCO_3 + 4.0GaO_{1.5}$	$LaCaGaO_4 + LaCaGa_3O_7 + CaO$
7	⊙	$1.0LaO_{1.5} + 6.0CaCO_3 + 5.0GaO_{1.5}$	$LaCaGa_3O_7 + CaO + Ca_5Ga_6O_{14}$
8	⊙	$0.5LaO_{1.5} + 4.5CaCO_3 + 5.5GaO_{1.5}$	$LaCaGa_3O_7 + CaO + Ca_5Ga_6O_{14}$
9	⊙	$0.4LaO_{1.5} + 2.0CaCO_3 + 3.2GaO_{1.5}$	$LaCaGa_3O_7 + Ca_5Ga_6O_{14} + Ca_3Ga_4O_9$
10	⊙	$0.5LaO_{1.5} + 2.5CaCO_3 + 4.5GaO_{1.5}$	$LaCaGa_3O_7 + Ca_3Ga_4O_9 + CaGa_2O_4$
11	⊙	$0.5LaO_{1.5} + 1.5CaCO_3 + 4.5GaO_{1.5}$	$LaCaGa_3O_7 + CaGa_2O_4 + CaGa_4O_7$
12	⊙	$0.5LaO_{1.5} + 1.0CaCO_3 + 4.0GaO_{1.5}$	$LaCaGa_3O_7 + CaGa_4O_7 + Ga2O_3$
A	△	$5.0LaO_{1.5} + 1.0CaCO_3 + 3.0GaO_{1.5}$	$LaCaGaO_{4+} La_4Ga_2O_9$
B	△	$4.0LaO_{1.5} + 2.0CaCO_3 + 4.0GaO_{1.5}$	$LaCaGaO_4 + LaGaO_3$
C	△	$2.0LaO_{1.5} + 2.0CaCO_3 + 4.0GaO_{1.5}$	$LaCaGaO_4 + LaCaGa_3O_7$
D	△	$2.0LaO_{1.5} + 6.0CaCO_3 + 2.0GaO_{1.5}$	$LaCaGaO_4 + CaO$
E	△	$1.0LaO_{1.5} + 1.0CaCO_3 + 4.0GaO_{1.5}$	$LaCaGaO_4 + Ga_2O_3$
m1	▲	$2.0LaO_{1.5} + 1.0CaCO_3$	$La_2O_3 + CaO$
m2	▲	$1.0LaO_{1.5} + 1.0CaCO_3$	$La_2O_3 + CaO$
m3	▲	$1.0LaO_{1.5} + 2CaCO_3$	$La_2O_3 + CaO$
n1	▲	$3.0LaO_{1.5} + 1.0GaO_{1.5}$	$La_2O_3 + La_4Ga_2O_9$
n2	▲	$3.0LaO_{1.5} + 2.0GaO_{1.5}$	$La_4Ga_2O_9 + LaGaO_3$
n3	▲	$1.0LaO_{1.5} + 3.0GaO_{1.5}$	$LaGaO_3 + Ga_2O_3$
p1	▲	$7.0CaCO_3 + 6.0GaO_{1.5}$	$CaO + Ca_5Ga_6O_{14}$
p2	▲	$12.0CaCO_3 + 9.5GaO_{1.5}$	$Ca_5Ga_6O_{14} + Ca_3Ga_4O_9$
p3	▲	$2.5CaCO_3 + 4.0GaO_{1.5}$	$Ca_3Ga_4O_9 + CaGa_2O_4$
p4	▲	$1.5CaCO_3 + 4.0GaO_{1.5}$	$CaGa_2O_4 + CaGa_4O_7$
p5	▲	$1.0CaCO_3 + 5.0GaO_{1.5}$	$CaGa_4O_7 + Ga_2O_3$
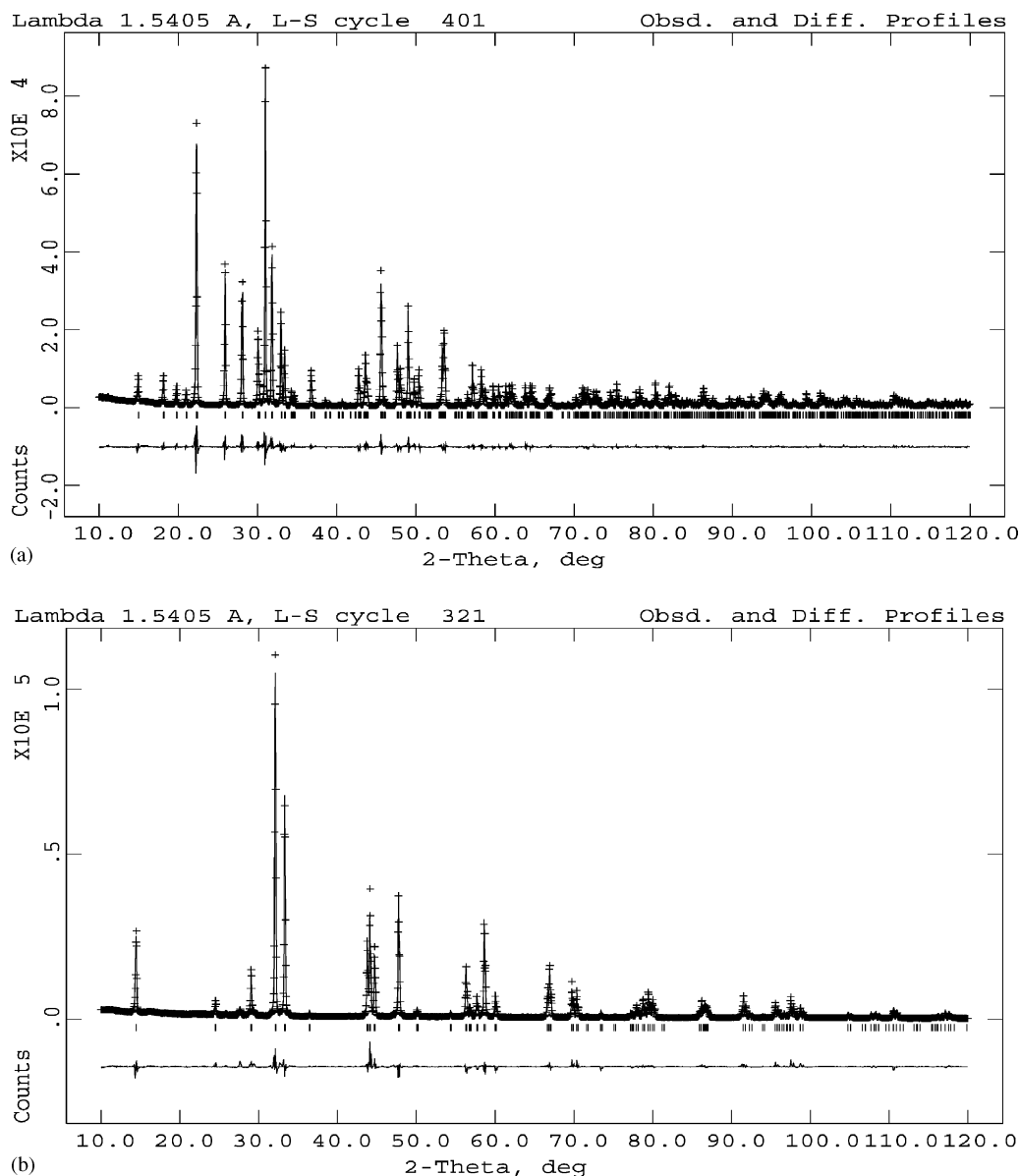
Fig. 2. The observed and fitting X-ray diffraction patterns of the o-LaCaGaO$_4$ and t-LaCaGaO$_4$. (a) o-LaCaGaO$_4$ fitted by the model using space group $Pna2_1$ and (b) t-LaCaGaO$_4$ fitted by the model using space group $I4mm$.

In addition to the binary phases, two known ternary compounds, LaCaGaO$_4$ and LaCaGa$_3$O$_7$, were identified in the La$_2$O$_3$–CaO–Ga$_2$O$_3$ system. The whole phase diagram is basically divided into a member of three-phase regions by the ternary compounds. The solid solution limit of CaO in LaGaO$_3$ may be too small (less than 0.5%) to be observed by our X-ray diffraction method. It has not been found under our synthesis condition and testing method. The crystal structures of both ternary compounds were reported. LaCaGa$_3$O$_7$ crystallizes in tetragonal structure in the space group $P\bar{4}2_1m$ [43]. LaCaGaO$_4$ was known to crystallize in K$_2$NiF$_4$ (t-LaCaGaO$_4$) and olivine-type structure (o-LaCaGaO$_4$) [44]. The olivine-type

LaCaGaO$_4$ could be readily obtained at 1150°C, so it appears in the phase diagram as a fundamental component. The t-LaCaGaO$_4$ phase can only be obtained by air-quenching the o-LaCaGaO$_4$ sample from 1350°C. In Fig. 2, we show the powder X-ray diffraction patterns of both o- and t-LaCaGaO$_4$ with the corresponding fitting.

The olivine (Mg,Fe)$_2$SiO$_4$ itself is the main constituent of the upper mantle. It is well recognized that the olivine may transform to the spinel structure under high pressure because of the density difference. The pressure-induced olivine–spinel phase transition has been studied extensively, and about 10% density change that is believed to be the driving force of the phase transition
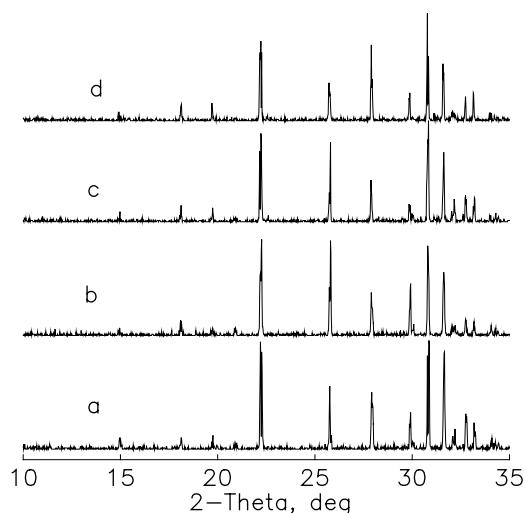
Fig. 3. The In situ X-ray diffraction patterns of the o-LaCaGaO$_4$ at 1210. (a) X-ray diffraction patterns when the o-LaCaGaO$_4$ was heated up to 1210°C from room temperature in 6 h, (b) X-ray diffraction patterns after the o-LaCaGaO$_4$ was kept at 1210°C for 12 h, (c) X-ray diffraction patterns after the o-LaCaGaO$_4$ was kept at 1210°C for 36 h, and (d) X-ray diffraction patterns after the o-LaCaGaO$_4$ was kept at 1210°C for 60 h.

Fig. 5. The normalized unit-cell volume of t-LaCaGaO$_4$ and o-LaCaGaO$_4$ at different temperatures. ($\triangledown$) the data obtained when t-LaCaGaO$_4$ were cooled down from higher temperature; (O) the data obtained when t-LaCaGaO$_4$ were heated up from lower temperature.
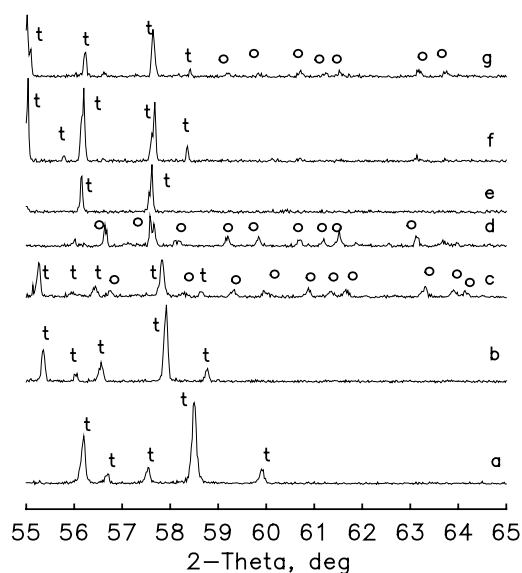

Fig. 4. The In situ X-ray diffraction patterns of the t-LaCaGaO4 at different temperatures (a) 27°C, (b) 900°C raising from a lower temperature, (c) 1000°C raising from 900°C, (d) 1200°C raising from 1000°C, (e) 1220°C raising from 1200°C, (f) 1150°C cooling from 1220°C and (g) 1100°C cooling from 1150°C. t is t–LaCaGaO4, o is o-LaCaGaO$_4$.

was observed [45,46]. The in situ powder X-ray diffraction study shows that the o-LaCaGaO$_4$ maintains stability below 1210°C as shown in Fig. 3. However, as shown in Fig. 4, the t-LaCaGaO$_4$ just maintains stability below 900°C, changes to o-LaCaGaO$_4$ above 1000°C and transforms to t-LaCaGaO$_4$ at 1220°C, which can be stable at 1150°C when it is cooled from 1220°C and becomes the o-LaCaGaO$_4$ when the temperature is
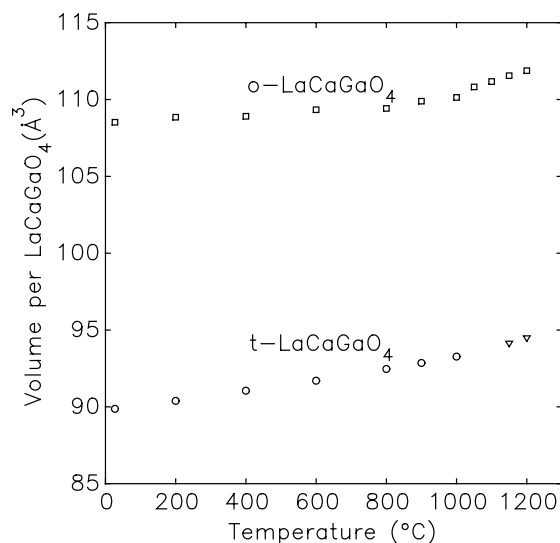
lower than 1100°C. Fig. 5 shows the normalized unit-cell volume of the LaCaGaO$_4$ phases at different temperatures. The normalized unit-cell volume of o-LaCaGaO$_4$ is about 20% larger than t-LaCaGaO$_4$ and that implies the olivine structure is indeed a low-pressure modification of this compound.

Most of the $LnMA$O$_4$ compounds (Ln = rare earth, M = Ba, Sr, Ca, A = Ga, Al) [16–31] were reported to crystallize in ideal K$_2$NiF$_4$-type structure and described in the space group of $I4/mmm$. Vasilechko et al. [44] suggested that the t-LaCaGaO$_4$ might also crystallize in the space group of $I4mm$ besides $I4/mmm$, but they finally chose the $I4/mmm$ space group for t-LaCaGaO$_4$ because $I4mm$ did not improve the structure refinement. As far as the atomic coordination is concerned, both models are similar and, it is difficult to differentiate them merely by crystallographic means. In fact, both structure models fit the powder X-ray diffraction pattern equally well as shown in Table 2. However, the space group $I4mm$ allows the Ga atoms deviate from the center of the octahedra, which leads to spontaneous polarization phenomenon. The t-LaCaGaO$_4$ indeed shows electric hysteresis behavior as shown in Fig. 6 indicating that the space group of $I4mm$ is more appropriate. The octahedra are elongated along the 4-fold axis in both models, but the gallium atoms are significantly deviated from the center of the octahedra in the $I4mm$ model resulting in ferroelectric property.

The ideal olivine-type structure of α-NdCaGaO$_4$ was described in the orthorhombic space group of $Pnma$ [35]. In the structure as shown in Fig. 7, oxygen atoms form hexagonal closed packing along the b-axis, gallium atoms occupy the tetrahedral sites and other cations

Table 2
The comparison of the different model for t-LaGaO$_4$

	Structure model		
Space group	$I4mm$ (this work)	$I4/mmm$ (this work)	$I4/mmm$ (16)
a(Å)	3.8187(1)	3.8177(1)	3.8160(2)
c(Å)	12.3477(1)	12.3477(1)	12.343(1)
La/Ca1	0, 0, 0.3465(1)	0, 0, 0.3579(3)	0, 0, 0.3605(4)
La/Ca2	0, 0, −0.3695(1)		
Ga	0, 0, 0^a	0, 0, 0	0, 0, 0
O1	0, 1/2, −0.0131(1)	0, 1/2, 0	0, 1/2, 0
O2	0, 0, 0.1501(1)	0, 0, 0.1651(2)	0, 0, 0.166(2)
O3	0, 0, −0.1834(1)		
R	$R_{wp} = 0.11$, $R_p = 0.078$	$R_{wp} = 0.11$, $R_p = 0.078$	$R_I = 0.0696$
Ga–O1 × 4	1.9161(1)	1.9093(1)	1.9080(2)
Ga–O2	1.8531(1)	2.0388(1) × 2	2.05(3) × 2
Ga–O3	2.2645(2)		

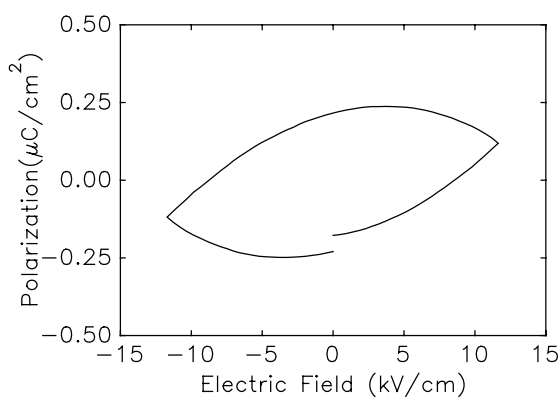^{a} The Ga atom is chosen as the origin in this space group.

Fig. 6. The D–E hysteresis loop of the t-LaCaGaO$_4$ at room temperature.

occupy the octahedral sites. The X-ray diffraction patterns of o-LaCaGaO$_4$ are very similar to α-NdCa GaO$_4$, this implies that it should be isostructural to α-NdCaGaO$_4$. However, the structure of o-LaCaGaO$_4$ can also be described in the polar space group $Pna2_1$ without changing the reflection conditions. One would expect that both structure models have similar atomic coordinates and, also, diffraction patterns, which could not be differentiated merely by structure determination. Table 3 lists the results of the Rietveld refinement for the two structure models including the crystallographic data and atomic coordinates and, one can see that the refinements for both models are equally well. The D–E hysteresis loop measurement indicates that o-LaCa
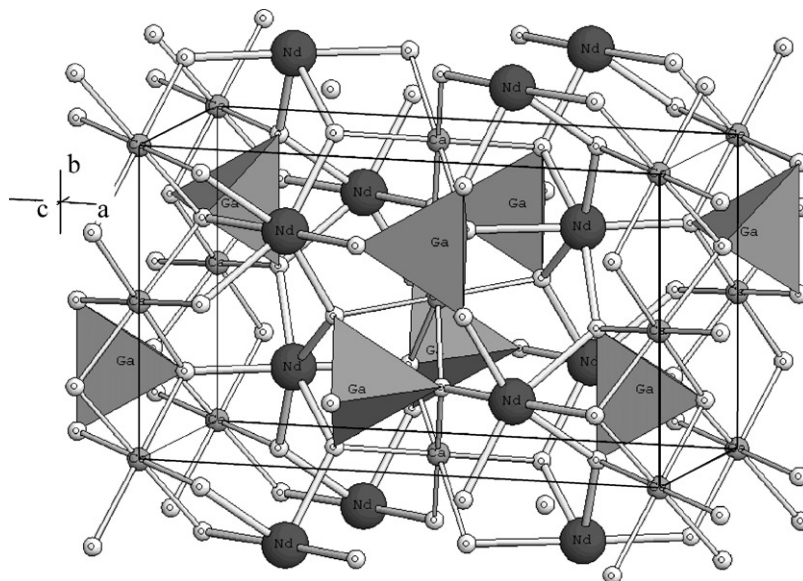

Fig. 7. The structure of α-NdCaGaO$_4$. The GaO$_4$ is expressed as tetrahedron and Nd and Ca are expressed as large and small balls, respectively.

Table 3
The comparison of the different space group suggested for o-LaGaO$_4$

	Structure model	
Space group	Pnma	Pna2$_1$
La1	0.220(1), 0.250, 0.511(1)	0.216(1), 0.508(1), 0.244(1)
Ga1	0.410(1), 0.250, 0.069(1)	0.406(1), 0.066(1), 0.243(1)
Ca1	0.500, 0.500, 0.500	0.500, 0.500, 0.500[a]
O1	0.548(1), 0.250, 0.226(1)	0.545(1), 0.224(1), 0.236(1)
O2	0.411(1), 0.250, 0.724(1)	0.407(1), 0.722(1), 0.234(1)
O3	0.341(1), 0.459(1), 0.232(1)	0.335(1), 0.226(1), 0.436(1)
O4		0.154(1), 0.732(2), 0.517(2)
R	$R_{wp} = 0.097$, $R_p = 0.071$	$R_{wp} = 0.097$, $R_p = 0.071$
a(Å)	11.8083(1)	11.8083(1)
b(Å)	6.8603(1)	5.3529(1)
c(Å)	5.3529(1)	6.8603(1)
Ga–O1	1.8373(1)	1.8375(1)
Ga–O2	1.8439(1)	1.8430(1)
Ga–O3	1.8676(1)−2	1.7909(1)
Ga–O4		1.959(11)

[a] The Ca atom is chose as the relative origin of this space group.
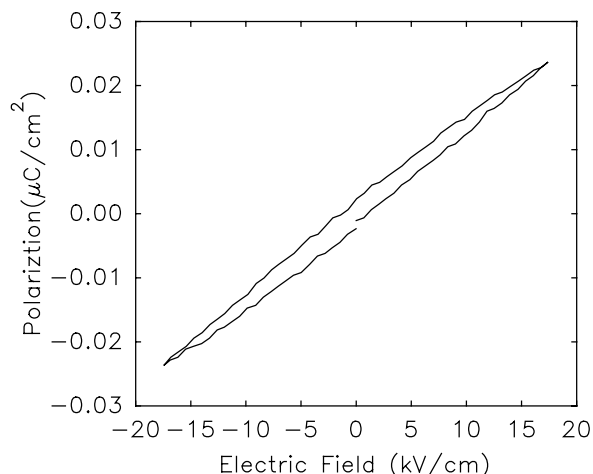
Fig. 8. The D–E hysteresis loop of the o-LaCaGaO$_4$ at room temperature.

Fig. 9. The conductivity of o- and t-LaCaGaO$_4$ at different temperatures.

GaO$_4$ also shows weak hysteresis behavior (Fig. 8) indicating that the appropriate space group is the Pna2$_1$.

Both o-LaCaGaO$_4$ and t-LaCaGaO$_4$ are isolators with rather low conductivity. Fig. 9 shows the temperature dependence of the conductivity for both phases. The conductivity is about $2.44 \times 10^{-8} \Omega^{-1} cm^{-1}$ for t-LaCaGaO$_4$ and $1.44 \times 10^{-9} \Omega^{-1} cm^{-1}$ for o-LaCaGaO$_4$ at 440°C. The activation energies are about 1.08 and 1.20 eV, respectively, which implies that the conductivity of the o- and t-LaCaGaO$_4$ may be related to deficiency in oxygen content. Because only single semicircle is observed in the impedance plot for all samples, the conductivity data shown in the figure are the total conductivity including the bulk and grain boundary [47]. According to the crystal structures, the polarizations in both t- and o-LaCaGaO$_4$ structures are all along the c-axis and, could be attributed to the spatial deviation of gallium atoms from the center of the octahedra
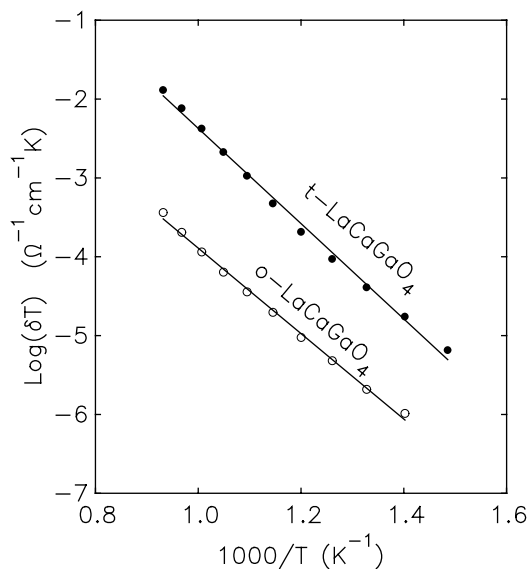
and the tetrahedra, respectively. The polarization of the o-LaCaGaO$_4$ is about one order of magnitude smaller than t-LaCaGaO$_4$. Considering the rigid nature of the tetrahedron, one could expect that the spontaneous polarization effect should be small for o-LaCaGaO$_4$. This effect can be roughly represented by the bond difference between Ga–O3 and Ga–O4 in o-LaCaGaO$_4$, which is rather small as compared with the bond difference between Ga–O2 and Ga–O3 in t-LaCaGaO$_4$.

In conclusion, two crystal forms of LaCaGaO$_4$ were obtained. The tetragonal LaCaGaO$_4$ was synthesized at 1350°C with quenching to room temperature, crystallized in space group I4mm and can be stable below 900°C. The orthorhombic LaCaGaO$_4$ was synthesized at 1150°C without quenching, crystallized in space group Pna2$_1$ and can be stable under 1210°C. Both of the phases show ferroelectric behavior with low conductivity.

Acknowledgments

References

[1] T. Ishihara, H. Matsuda, Y. Takita, J. Am. Chem. Soc. 116 (1994) 3801.
[2] T. Ishihara, H. Matsuda, Y. Takita, Solid State Ionics 79 (1995) 147.
[3] K.Q. Huang, M. Feng, J.B. Goodenough, J. Am. Ceram. Soc. 79 (1996) 1100.
[4] K.Q. Huang, J.B. Goodenough, J. Solid State Chem. 136 (1998) 274–283.
[5] J.B. Goodenough, Nature 404 (2000) 821–823.

[6] J.W. Stevenson, T.R. Armstrong, D.E. McCready, L.R. Pederson, W.J. Weber, J. Electrochem. Soc. 144 (1997) 3613.

[7] A.C. Tas, P.J. Majewski, F. Aldinger, J. Am. Ceram. Soc. 83 (2000) 2954–2960.

[8] A. Skowron, P.N. Huang, A. Petric, J. Solid State Chem. 143 (1999) 202–209.

[9] T. Inagaki, K. Miura, H. Yoshida, J. Fujita, M. Nishimura, Solid State Ionics 118 (1999) 265–269.

[10] C.J. Howard, B.J. Kennedy, J. Phys.: Condens. Matter 11 (1999) 3229–3236.

[11] H. Hayashi, H. Inaba, M. Matsuyama, N.G. Lan, M. Dokiya, H. Tagawa, Solid State Ionics 122 (1999) 1–15.

[12] N. Maffei, A.K. Kuriakose, J. Power Sources 75 (1998) 162–166.

[13] P.J. Majewski, M. Rozumek, H. Schluckwerder, F. Aldinger, J. Am. Ceram. Soc. 84 (2001) 1093–1096.

[14] M. Hrovat, S. Bernik, J. Holc, Z. Samardzija, J. Mater. Res. 14 (1999) 2351–2354.

[15] M. Hrovat, Z. Samardzija, J. Holc, S. Bernik, J. Mater. Res. 14 (1999) 4460–4462.

[16] R. Sobolewski, P. Gierlowski, W. Kula, S. Zarembinski, S.J. Lewandowski, M. Berkowski, A. Pajaczkowska, B.P. Gorshunov, D.B. Lyudmirsky, O.I. Sirotinsky, IEEE Trans. Magn. 27 (1991) 876–879.

[17] R. Brown, V. Pendrick, D. Kalokitis, B.H.T. Chai, Appl. Phys. Lett. 57 (1990) 1351–1353.

[18] S. Hontsu, J. Ishii, T. Kawai, S. Kawai, Appl. Phys. Lett. 59 (1991) 2886–2888.

[19] A. Pajaczkowska, P. Byszewski, J. Cryst. Growth 128 (1993) 694–698.

[20] J. Fava, Yu.P. Udalov, J.-M. Reau, G. Le Flem, P. Hagenmuller, Compt. Rend. C 274 (1972) 1837–1839.

[21] G. Blasse, J. Inorg. Nucl. Chem. 27 (1965) 2683–2684.

[22] G. Nguyen-Trut-Dinh, J. Le Flem, A. Fava, G. Daoudi, Demazeau, J. Chim. Phys. 74 (1977) 965–970.

[23] J.P. Oudalov, A. Daoudi, J.C. Joubert, G. Le Flem, P. Hagenmuller, Bull. Soc. Chim. Fr. 10 (1970) 3408–3410.

[24] B.Ya. Brach, E.N. Glazacheva, N.A. Kostromina, R.M. Rakhmankulov, A.Yu. Romanov, Yu.P. Udalov, Inorg. Mater. (USSR) 23 (1987) 977–981.

[25] J.C. Joubert, A. Collomb, D. Emaleh, G. Le Flem, A. Daoudi, G. Ollivier, J. Solid State Chem. 2 (1970) 343–346.

[26] G. Blasse, J. Inorg. Nucl. Chem. 30 (1968) 656–658.

[27] L.M. Kovba, L.N. Lykova, E.V. Antipov, Koord. Khim. 11 (1985) 1574–1576.

[28] Yu.P. Udalov, P. Golba, G. Le Flem, Zh. Neorg. Khim. 22 (1977) 476–482.

[29] P. Byszewski, J. Domagala, J. Fink-Finowicki, A. Pajaczkowska, Mater. Res. Bull. 27 (1992) 483–490.

[30] R.D. Shannon, R.A. Oswald, J.B. Parise, B.H.T. Chai, P. Byszewski, A. Pajaczkowska, R. Sobolewski, J. Solid State Chem. 98 (1992) 90–98.

[31] S. Erdei, M. McNeal, S.J. Jang, L.E. Cross, A.S. Bhalla, F.W. Ainger, A. Dabkowski, H.A. Dabkowska, J. Cryst. Growth 174 (1997) 324–327.

[32] A. Pajaczkowska, A. Gloubokov, Prog. Cryst. Growth Charact. 36 (1998) 123–162.

[33] C.L. Jia, X.H. Zeng, X.X. Xi, K. Urban, Phys. Rev. B 64 (2001) 075416.

[34] M. Berkowski, J. Alloys Compds. 251 (1997) 1–6.

[35] A. Daoudi, G. Demazeau, G. Le Flem, Rev. Chim. Miner. 11 (1974) 327.

[36] A.C. Larson, R.B. von Dreele, Report LAUR 86-748, Los Alamos National Laboratory, 1985.

[37] H. Yamane, K. Ogawara, M. Omori, T. Hirai, J. Am. Ceram. Soc. 78 (1995) 2385–2390.

[38] E. Antic-Fidancev, M. Lemaitre-Blaise, M. Latroche, P. Porcher, J. Coutures, J.P. Coutures, J. Alloys Compds. 250 (1997) 342–346.

[39] A.I. Bilyi, V.A. Bruskov, Yu.N. Grin, P.Yu. Zavalii, V.V. Kravchishin, A.E. Nosenko, Kristallografiya 31 (1986) 1217–1219.

[40] B.V. Merinov, S.L. Londar, Ya.M. Zakharko, Kristallografiya 33 (1988) 242–244.

[41] Yu.Ya. Scolis, V.A. Levitskii, L.N. Lykova, T.A. Kalinina, J. Solid State Chem. 38 (1981) 10–18.

[42] J. Jeevaratnam, F.P. Glasser, J. Am. Ceram. Soc. 44 (1961) 563–566.

[43] J.M.S. Skakle, R. Herd, Powder Diffr. 14 (1999) 195–202.

[44] L.O. Vasilechko, A.A. Fedorchuk, D.I. Savitskii, A.O. Matkovskii, S.B. Ubizskii, Inorg. Mater. 31 (1995) 1128–1131.

[45] J.H. Chen, D.J. Weidner, J.B. Parise, M.T. Vaughan, P. Raterron, Phys. Rev. Lett. 86 (2001) 4072–4075.

[46] L. Chudinovskikh, R. Boehler, Nature 411 (2001) 574–577.

[47] J.C.C. Abrantes, J.A. Labrincha, J.R. Frade, Mater. Res. Bull. 35 (2000) 955–964.